Far-Ultraviolet Electric Linear Dichroism of Poly(γ-methyl L-glutamate) in Hexafluoro-2-propanol and the Peptide Band in the 187-250-nm Wavelength Region[1]

Kiwamu Yamaoka,* Kazuyoshi Ueda, and Isao Kosako

Contribution from the Faculty of Science, Hiroshima University, Hiroshima 730, Japan.
Received November 5, 1985

Abstract: Electric linear dichroism spectra of poly(γ-methyl L-glutamate), $[Glu(OMe)]_n$, with a weight-average molecular weight of 13.5×10^4 in hexafluoro-2-propanol at residue concentrations of 0.50, 1.27, and 3.01 mM were measured at 25 °C and at 17.8 kV/cm in the 187-250-nm region. From the dependence of reduced dichroism ($\Delta\epsilon/\epsilon$) on applied electric field up to 26.3 kV/cm at wavelengths of 208, 215, and 230 nm, the orientation factor at 17.8 kV/cm was estimated to be 0.554. The isotropic spectrum of the peptide chromophore could be decomposed into four component bands with the Gaussian band shape. The wavelength dependence of the saturated reduced dichroism $(\Delta\epsilon/\epsilon)_s$ was simulated with these four bands by assigning an appropriate angle θ to each band, where θ is the angle between the direction of a transition moment and the orientation axis, i.e., the helix axis, of the whole $[Glu(OMe)]_n$ molecule. The agreement between the observed and simulated $(\Delta\epsilon/\epsilon)_s$ values was excellent over the 187-250-nm region with the following parameters (ϵ_{max} in M^{-1} cm^{-1}, λ_{max} in nm, $|\theta|$ in deg): band 1 (50, 234, 55.6), band 2 (540, 220, 54.73), band 3 (1650, 204.9, 50.6), band 4 (4150, 190, 56.1). Bands 3 and 4 are polarized neither parallel ($\parallel$, $\theta = 0°$) nor perpendicular ($\perp$, $\theta = 90°$) to the helix axis. Thus, Moffitt's prediction on the splitting of the peptide band in the helical conformation into $\parallel$ and $\perp$ components could not be verified.

The spectroscopic properties of polypeptides and proteins in ordered and disordered conformations are principally derived from the important chromophore, i.e., the peptide bond, incorporated in the polymer backbone. Theoretical efforts have, therefore, been devoted to interpret numerous experimental results on the absorption and circular dichroism (CD) spectra of helical and random-coiled polypeptides. The interpretation is based on the Moffitt-Kirkwood-Tinoco theory,[2-4] which treats the polymer spectra as arising from the interaction of identical peptide chromophores. On the other hand, rigorous experimental tests of the theory are strangely scarce, though some experimental data discording to the theory have resulted from precise CD and other measurements.[2,3,5] Among consequences that are derived from the elegant theory, Moffitt's prediction on the split of the 190-nm peptide band into parallel- and perpendicular-polarized components[6,7] can be verified readily by experimental techniques.[3,5] A distinct shoulder near 205 nm in the absorption spectra of helical polypeptides in solutions was considered to be the evidence for the validity of Moffitt's exciton theory.[8,9] We must, however, be aware that this result reveals nothing about the polarization direction of transition moments.

An appropriate approach is the measurement of the anisotropic spectra of oriented helical polymers, as was first performed on the stroked poly(γ-methyl L-glutamate), $[Glu(OMe)]_n$, film.[10,11] Since the degree of orientation of helices in a bulk film cannot be quantitatively evaluated, the observed dichroism is only qualitative. Yet, an increase in the 205-nm absorption intensity was construed as being due to the parallel-polarized component of the split band.[8-11] In this case, however, any value between 0 and 54.7° could have been assigned to the angle between the transition moment direction and the *orientation axis*.[12,13] A more direct technique is the orientation of helix molecules in dilute solution by an externally applied electric field. Indeed, both electric dichroism and electric birefringence have been employed in studies of electric, optical, and hydrodynamic properties of helical polypeptides.[14,15] Mandel and Holzwarth were the first who investigated the far-ultraviolet linear and circular dichroism of $[Glu(OMe)]_n$ helices oriented in hexafluoro-2-propanol (HFP) by electric field.[16] They were unable to determine the degree of orientation of helices but assigned the 187.8- and 205.4-nm bands to the perpendicular- and parallel-polarized components of the π-π^* peptide band, respectively.

In order to clarify the exciton band splitting and other spectroscopic characteristics of the peptide chromophore in helical polymers, we have lately initiated the far-ultraviolet electric linear dichroism (ELD) study of various biopolymers, with emphasis on the quantitative interpretation of the observed dichroism data.[17,18] In a preliminary report,[17] we showed that the peptide spectrum of poly(α-L-glutamic acid), $(Glu)_n$, contains at least three transition moments with the polarization directions very different from Moffitt's predicted values. Surprisingly, this finding was common to $(Glu)_n$, in either the *helical* or *random-coiled* conformation,[17] and collagen.[18] Being stimulated by these unexpected results, we now extend our ELD study to $[Glu(OMe)]_n$ in HFP. This system is suitable for the present purpose because HFP is transparent in the far-ultraviolet region and electrically nonconducting; thus, the degree of molecular orientation can be evaluated unambiguously at a given electric field strength with the classical theory of field orientation.[19-21] Fortunately, the electrooptical

(1) Far-Ultraviolet Electric Linear Dichroism. 3. Part 2: ref 18. This work was supported in part by a Grant-in-Aid for Scientific Research (Grant No. 347009) from the Ministry of Education, Science, and Culture of Japan.
(2) Woody, R. W. *J. Polym. Sci., Macromol. Rev. Ed.* **1977**, *12*, 181-320. Numerous references are cited in this comprehensive review.
(3) Charney, E. *The Molecular Basis of Optical Activity*; Wiley: New York, 1979.
(4) Schellman, J. A.; Becktel, W. J. *Biopolymers* **1983**, *22*, 171-187.
(5) These points are well summarized in: Woody, R. W. *J. Polym. Sci., Macromol. Rev. Ed.* **1977**, *12*, 206-257. Reference 3, Chapters 7 and 8, pp 234-237 and 289-291, respectively.
(6) Moffitt, W. *Proc. Natl. Acad. Sci. U.S.A.* **1956**, *42*, 736-746.
(7) Moffitt, W. *J. Chem. Phys.* **1956**, *25*, 467-478.
(8) Tinoco, I., Jr.; Halpern, A.; Simpson, W. T. In *Polyamino Acids, Polypeptides, and Proteins*; Stahmann, M. A., Ed.; University of Wisconsin: Madison, 1962; pp 147-157.
(9) Rosenheck, K.; Doty, P. *Proc. Natl. Acad. Sci. U.S.A.* **1961**, *47*, 1775-1785.
(10) Gratzer, W. B.; Holzwarth, G. M.; Doty, P. *Proc. Natl. Acad. Sci. U.S.A.* **1961**, *47*, 1785-1791.
(11) Holzwarth, G.; Doty, P. *J. Am. Chem. Soc.* **1965**, *87*, 218-228.
(12) Charney, E.; Milstien, J. B.; Yamaoka, K. *J. Am. Chem. Soc.* **1970**, *92*, 2657-2664.
(13) Yamaoka, K.; Charney, E. *Macromolecules* **1973**, *6*, 66-76.
(14) Paulson, C. M., Jr. In *Molecular Electro-Optics, Part 1*; O'Konski, C. T., Ed.; Marcel Dekker: New York, 1976; Chapter 7. References are cited therein prior to 1972.
(15) Yoshioka, K. In *Molecular Electro-Optics, Part 2*; O'Konski, C. T., Ed.; Marcel Dekker: New York, 1978; Chapter 17. References are cited therein prior to 1973.
(16) Mandel, R.; Holzwarth, G. *J. Chem. Phys.* **1972**, *57*, 3469-3477.
(17) Yamaoka, K.; Ueda, K.; Asato, M. *J. Am. Chem. Soc.* **1984**, *106*, 3865-3866.
(18) Yamaoka, K.; Asato, M.; Matsuda, K.; Ueda, K. *Bull. Chem. Soc. Jpn.* **1984**, *57*, 1771-1776.
(19) O'Konski, C. T.; Yoshioka, K.; Orttung, W. H. *J. Phys. Chem.* **1959**, *63*, 1558-1565.
(20) Yamaoka, K.; Charney, E. *J. Am. Chem. Soc.* **1972**, *94*, 8963-8974.
(21) Yamaoka, K.; Ueda, K. *J. Phys. Chem.* **1982**, *86*, 406-413.

0002-7863/86/1508-4619$01.50/0

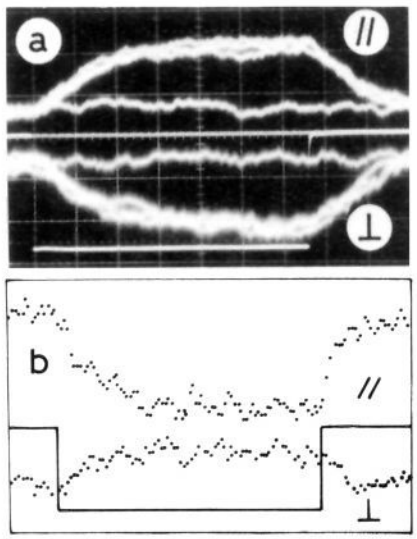

Figure 1. Typical dichroism signals of $[Glu(OMe)]_n$ in HFP. (a) Photographed signals at 208 nm; three traces for signals polarized parallel (∥) and perpendicular (⊥) to the direction of external field. The vertical scales are 20 mV/division for ∥ and ⊥. The sweep time is 200 μs/division. The field strength of pulse is 26.3 kV/cm. (b) Digitized signals at 230 nm; 16 ∥ and ⊥ signals averaged. Each dot represents a 0.5-μs sampling time at a field strength of 21.5 kV/cm.

and conformational aspects of $[Glu(OMe)]_n$ in HFP were recently investigated and thoroughly characterized by reversing-pulse electric birefringence.[22,23] From the quantitative measurement of reduced dichroism over the 187–250-nm region, we can now conclude the presence of four component bands in the peptide absorption spectrum and discuss the disparity between the experimental result and Moffitt's prediction.

Experimental Section

Materials. Poly(γ-methyl L-glutamate) is the third fraction, which was purified from a high molecular weight sample (Pilot Chemicals) by the successive precipitation method.[24] The intrinsic viscosity $[\eta]$ in dichloroacetic acid was 267 $cm^3\ g^{-1}$ at 25 °C.[22] The weight-average molecular weight M_w was estimated to be 13.5×10^4 from a $[\eta]$ vs. M_w relationship.[25] 1,1,1,3,3,3-Hexafluoro-2-propanol (HFP) for spectroscopy (Merck) was used without further purification.

Electric Linear Dichroism Apparatus. A pulsed square-wave ELD apparatus was constructed in this laboratory. The principles and the design procedure were reported in previous papers.[12,13,26,27] The detailed description and performance of the present far-ultraviolet apparatus were recently given elsewhere.[18] It consists of an electric pulsing system, which can deliver a single square-wave pulse with a variable duration between 10 μs and 5 ms and a field strength up to 26.5 kV/cm,[26] and a new optical system, which is composed of a double-grafting monochromator, a 200-W deuterium discharge arc lamp, and a magnesium fluoride beam-splitting polarizer to cover the 185–360-nm region.[18] A special feature added to this ELD apparatus is the simultaneous and independent detection of parallel and perpendicular dichroism signals by a single electric pulse externally applied to a sample solution. These two signals and an attenuated electric pulse could be displayed simultaneously on a cathode ray tube of a dual-beam oscilloscope and photographed with a camera.[18]

After completion of the far-ultraviolet measurement between 187 and 230 nm, it was further suspected that a very weak absorption band could possibly be hidden in the 230–250-nm region. Because of weak dichroism signals, the photographic recording was abandoned. The measurement between 210 and 250 nm was then performed on another apparatus, which can detect either a parallel or perpendicular signal separately,[26,27] in conjunction with a digitized signal detection system.[22,23] With this transient-wave memory microcomputer system, signals can be accumulated in arbitrary numbers, stored, and then averaged to improve signal-to-noise ratios. Usually 16, occassionally up to 64, repeated signals were taken at each wavelength for averaging. The $[Glu(OMe)]_n$ helix in HFP was stable enough to withstand such repeated pulses, probably because of low conductivity of HFP. Figure 1 shows two types of dichroism signals: one photographic and the other digitized.

Measurement. A $[Glu(OMe)]_n$ sample, dried at 78 °C for 8 h under reduced pressure, was dissolved in HFP to prepare three solutions, the concentrations of which are 0.50 (187–230.5 nm), 1.27 (214–238 nm), and 3.01 mM (215–250 nm) in terms of monomer (residue) unit. The "Kerr" cells, made of Kel-F, were equipped with stainless or gold-plated brass electrodes.[12,13,26,27] The path length (cm), the electrode gap (cm), and the wavelength region (nm) are, respectively, as follows: (1) at 0.50 mM (0.60, 0.327, 187–208), (1.00, 0.207, 200.5–217), (2.00, 0.330, 210–250); (2) at 1.27 mM (2.00, 0.330, 214–238); (3) at 3.01 mM (2.00, 0.330, 215–250). All measurements were carried out at 25 ± 0.05 °C under nitrogen gas purge (3 L/min). The isotropic absorption spectra in the absence of electric field were measured on a Hitachi EPS-3T recording spectrophotometer with a matched pair of quartz cells, the path lengths being 0.5, 1.0, and 2.0 cm.

Data Analysis. For the linearly polarized light beam with the polarization vector parallel to the direction of externally applied electric field, the difference in absorbances, $\Delta A_\parallel$, is defined as $\Delta A_\parallel = A_\parallel^E - A = \Delta\epsilon_\parallel C_p d$. Similarly for the perpendicularly polarized light, $\Delta A_\perp = A_\perp^E - A = \Delta\epsilon_\perp C_p d$, where C_p is the residue concentration of $[Glu(OMe)]_n$, d is path length, $A_\parallel^E$, $A_\perp^E$, and A are the field-on and field-off absorbances, and ϵ's are the corresponding molar absorption coefficients.[12,13,26,27] The reduced dichroism is defined as $\Delta A/A = (A_\parallel^E - A_\perp^E)/A$ or $\Delta\epsilon/\epsilon = (\epsilon_\parallel^E - \epsilon_\perp^E)/\epsilon$ and can be calculated from the observed quantities. If an external pulse field orients solute molecules, inducing no conformational transition, the relationship in eq 1 should hold.[20] Hence, the field-off isotropic spectrum A can be calculated from the field-on anisotropic spectra $A_\parallel^E$ and $A_\perp^E$.

$$\Delta A_\parallel/A = -2\Delta A_\perp/A \qquad 3A = A_\parallel^E + 2A_\perp^E \tag{1}$$

If the polymer molecules are in a particular helical conformation, the reduced dichroism for the ith optical transition at a given wavelength λ is expressed as[27] in eq 2, where Φ is the orientation function[19,20] or the

$$\frac{\Delta A}{A} = \frac{\sum_i \Delta A_i}{\sum_i A_i} = \tfrac{3}{2}\left\{\frac{\sum_i (3\cos^2\theta_i - 1)A_i}{\sum_i A_i}\right\}\Phi \tag{2}$$

orientation factor at a given field strength E, θ_i is the angle between the direction of the ith optical transition moment and the orientation axis of the whole molecule, and A_i is the absorbance at λ of the ith component band. For a cylindrically symmetric helix molecule, the orientation axis coincides with the helix axis. In this case, the orientation function approaches unity at infinitely high electric field. The saturated reduced dichroism, $(\Delta A/A)_s$, can be derived from eq 2 to be as in eq 3, where $(\Delta A/A)_E$ is the reduced dichroism observed at a given field strength E and wavelength λ and Φ_E is the orientation factor at E, the latter being independent of λ.

$$\left(\frac{\Delta A}{A}\right)_s = \left(\frac{\Delta A}{A}\right)_E \left(\frac{1}{\Phi}\right)_E = \tfrac{3}{2}\frac{\sum_i (3\cos^2\theta_i - 1)A_i}{\sum_i A_i} \tag{3}$$

Results and Discussion

Dependence of Linear Dichroism on Wavelength. Figure 2 shows the experimental data taken over the 187–250-nm region at a constant applied field strength of 17.8 kV/cm. From parallel and perpendicular dichroism signals, the steady-state or equilibrium values, $\Delta\epsilon_\parallel$ and $\Delta\epsilon_\perp$, could be obtained separately (middle of Figure 2). This technique is essential to detect any possible conformational change induced by applied electric fields (cf. eq 1) and is definitely advantageous over the measurement of the difference only, i.e., the dichroism $\Delta\epsilon = \epsilon_\parallel - \epsilon_\perp$.[6,28,29] Within experimental errors, values of $\Delta\epsilon_\parallel$ and $-2\Delta\epsilon_\perp$ at each wavelength are equal to each other over the entire wavelength region; hence, eq 1 holds for $[Glu(OMe)]_n$ in HFP at 17.8 kV/cm. This result is strong support that the conformation of $[Glu(OMe)]_n$ remains

(22) Ueda, K. *Bull. Chem. Soc. Jpn.* **1984**, *57*, 2703–2711.
(23) Yamaoka, K.; Yamamoto, S.; Ueda, K. *J. Phys. Chem.* **1985**, *89*, 5192–5197.
(24) Yamaoka, K. Ph.D. Dissertation, University of California, Berkeley, CA, 1964.
(25) Okamoto, Y.; Sakamoto, R. *Nippon Kagaku Zasshi* **1969**, *90*, 669–672.
(26) Yamaoka, K.; Matsuda, K. *J. Sci. Hiroshima Univ., Ser. A: Phys. Chem.* **1980**, *43*, 185–203.
(27) Yamaoka, K.; Matsuda, K. *Macromolecules* **1981**, *14*, 595–601.
(28) Allen, F. S.; Van Holde, K. E. *Rev. Sci. Instrum.* **1970**, *41*, 211–216.
(29) Mandel, R.; Holzwarth, G. *Rev. Sci. Instrum.* **1970**, *41*, 755–758.

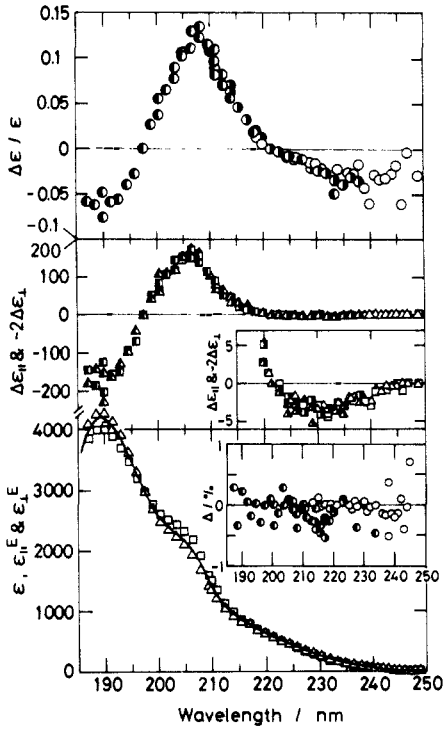

Figure 2. Wavelength dependence of linear dichroism of $[Glu(OMe)]_n$ in HFP at a constant field strength of 17.8 kV/cm. Top: (the reduced dichroism, $\Delta\epsilon/\epsilon$) (○) 3.01, (◑) 1.27, (●) 0.50 mM. Middle: (the parallel dichroism, $\Delta\epsilon_\parallel$) (□) 3.01, (▣) 1.27, (■) 0.50 mM; (the perpendicular dichroism multiplied by a factor of -2, $-2\Delta\epsilon_\perp$) (△) 3.01, (▲) 1.27, (▲) 0.50 mM. Bottom: the field-on absorption spectra $\epsilon_\parallel^E$ (□) and $\epsilon_\perp^E$ (△) and the field-off isotropic spectrum ϵ (—) [inset, the percent deviation of the calculated absorption spectrum ϵ_{calcd} from the observed one ϵ, i.e., $\Delta \equiv [(\epsilon_{calcd}/\epsilon) - 1] \times 100$: (○) 3.01, (◑) 1.27, (●) 0.50 mM].

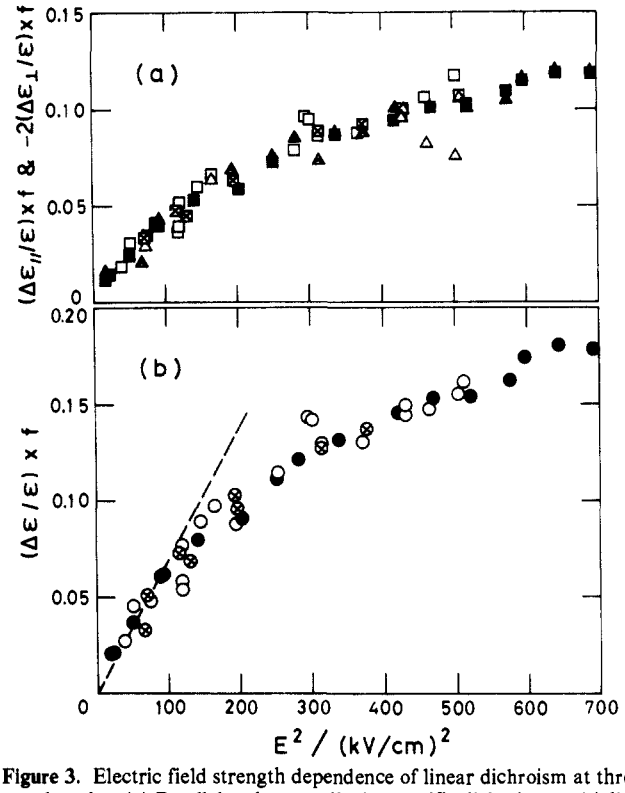

Figure 3. Electric field strength dependence of linear dichroism at three wavelengths. (a) Parallel and perpendicular specific dichroism multiplied by an appropriate factor f: (at 208 nm) (■) $(\Delta\epsilon_\parallel/\epsilon)f$, (▲) $(-2\Delta\epsilon_\perp/\epsilon)f$, $f = 1.0$; (at 215 nm) (⊠) $(\Delta\epsilon_\parallel/\epsilon)f$, (▲) $(-2\Delta\epsilon_\perp/\epsilon)f$, $f = 5.7$; (at 230 nm) (□) $(\Delta\epsilon_\parallel/\epsilon)f$, (△) $(-2\Delta\epsilon_\perp/\epsilon)f$, $f = -8.0$. (b) Reduced dichroism $\Delta\epsilon/\epsilon$ multiplied by the same factor as above: ● at 208 nm; ⊗ at 215 nm; ○ at 230 nm.

stable, once the molecular orientation, or the steady state, is completed. It should be noted that $\Delta\epsilon_\parallel$ and $\Delta\epsilon_\perp$ values are independent of concentrations of $[Glu(OMe)]_n$ between 0.50 and 3.01 mM. Thus, neither are molecular aggregates formed in HFP in accord with a previous electric birefringence result[22] nor do the path length and electrode gap of Kerr cells affect experimental values.

At the bottom of Figure 2, the parallel and perpendicular spectra, $\epsilon_\parallel^E$ and $\epsilon_\perp^E$, at a constant electric field are compared with the isotropic absorption spectrum, ϵ, observed in the absence of the field. This spectrum shows a peak at 189 nm and two distinct shoulders at about 205 and 220 nm, trailing on the longer wavelength side. The molar absorption coefficient, ϵ, at 189 nm is 4200 (M^{-1} cm^{-1}), which is in good agreement with previous values of 4060 at 187.8 nm[16] and 4350 at 188.5 nm.[30] In the inset, the observed value of ϵ is compared with the ϵ value calculated from $\epsilon_\parallel^E$ and $\epsilon_\perp^E$ (cf. eq 1). The deviation is very small and random, being only ±0.5% at most over the entire spectral range. This indicates that the field-on and field-off absorption spectra are essentially identical with each other.

Values of reduced dichroism were calculated from $\epsilon_\parallel^E$, $\epsilon_\perp^E$, and ϵ and are plotted on the top of Figure 2. The wavelength dependence of $\Delta\epsilon/\epsilon$ is unexpectedly complex; $\Delta\epsilon/\epsilon$ values are negative between 187 and 197 nm with a minimum (or plateau) near 190 nm, becoming positive above 197 nm with a maximum at about 208 nm and then decreasing to be negative at 222 nm. This general feature has already been observed for $(Glu)_n$, another helical polymer, in aqueous solutions; our preliminary report revealed that the peptide chromophore is associated with, at least, three different optical transitions between 187 and 230 nm.[17] Figure 2, surprisingly, shows that an additional transition should be present on the longer wavelength side between 230 and 250 nm. This is evidenced from the $\Delta\epsilon/\epsilon$ vs. λ plot, which shows a stepwise change between 227 and 234 nm; $\Delta\epsilon/\epsilon$ is ca. -0.01 at 227 nm but -0.03 above 234 nm. Thus, four, rather than three as previously believed, component bands (two strong and two weak ones) are involved in the peptide chromophore of $[Glu(OMe)]_n$ in the helical conformation (details will be discussed later). A precautionary comment is appropriate here: clearly, it is the wavelength dependence of *the reduced dichroism* $\Delta\epsilon/\epsilon$ (top of Figure 2), but not *the dichroism* $\Delta\epsilon$ *per se* (middle of Figure 2), that reveals the correct number of transition moments with different angles, θ_i (eq 2 or 3).[17,20] This fact has often been overlooked.[9,10,16,31]

Dependence of Linear Dichroism on Field Strength. The difficult but important procedure needed for a quantitative interpretation of the wavelength dependence of the ELD data is the evaluation of the average degree of orientation (or the orientation factor) of $[Glu(OMe)]_n$ helices at a given field strength. (Mandel and Holzwarth have ignored this procedure.[16]) For this purpose, the linear dichroism must first be measured over a wide, particularly medium-to-high, field strength range. Figure 3 shows the field strength dependence of $\Delta\epsilon/\epsilon$ values obtained at three wavelengths. At each wavelength, both $\Delta\epsilon_\parallel/\epsilon$ and $-2\Delta\epsilon_\perp/\epsilon$ values are practically equal to each other (Figure 3a); thus, eq 1 holds not only over the entire wavelength region but also over the entire field strength range (0–23.6 kV/cm). This result is important because it confirms that no breakdown of the helical structure of $[Glu(OMe)]_n$ occurs at field strengths above 17.8 kV/cm. The concentration effect is also negligible, since both $\Delta\epsilon_\parallel/\epsilon$ and $-2\Delta\epsilon_\perp/\epsilon$ at three different concentrations can be brought onto a smooth curve by multiplying the appropriate factors, f.

From values of $\Delta\epsilon_\parallel/\epsilon$ and $\Delta\epsilon_\perp/\epsilon$, the reduced dichroism was calculated and is plotted against E^2 in Figure 3b. The observed points are linear to the second power of field strength (dashed line) at low fields ($E \leq 8$ kV/cm), showing that the "Kerr law" is obeyed. $\Delta\epsilon/\epsilon$ values at higher fields tend to saturate, but the

(30) Parrish, J. R., Jr.; Blout, E. R. *Biopolymers* **1971**, *10*, 1491–1512.

(31) Mandel, R.; Holzwarth, G. *Biopolymers* **1973**, *12*, 655–674.

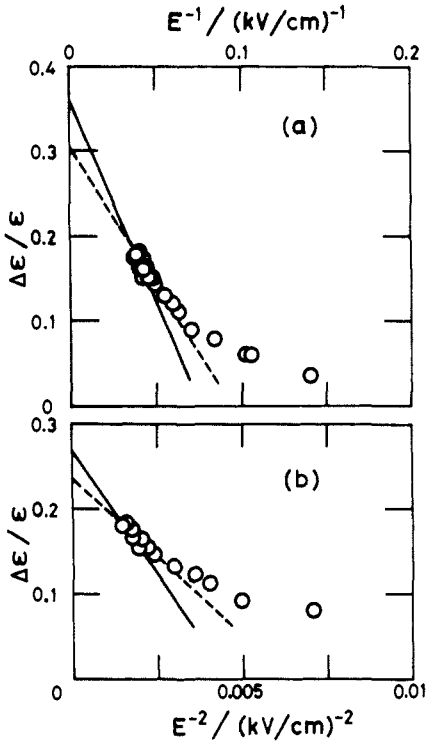

Figure 4. Extrapolation of $\Delta\epsilon/\epsilon$ values at 208 nm to infinitely high field strength: (a) $\Delta\epsilon/\epsilon$ vs. E^{-1}; (b) $\Delta\epsilon/\epsilon$ vs. E^{-2}. Linear extrapolations with highest five experimental $\Delta\epsilon/\epsilon$ values (—) and eight values (---).

highest value is unexpectedly small ($\Delta\epsilon/\epsilon$ at 208 nm $\doteq$ 0.18 even at the highest applied field of 26.3 kV/cm).

Saturated Reduced Dichroism and the Degree of Orientation. The saturated dichroism $(\Delta\epsilon/\epsilon)_s$ may be evaluated by a proper extrapolation of $\Delta\epsilon/\epsilon$ values observed at a given wavelength to infinitely high field. This extrapolation is usually performed by plotting $\Delta\epsilon/\epsilon$ values against E^{-1} or E^{-2} (the extrapolation procedure).[17,18,32-34] Figure 4 shows $\Delta\epsilon/\epsilon$ values at 208 nm plotted against E^{-1} (upper half) and against E^{-2} (lower half). It is immediately clear that a great difficulty is associated with this extrapolation procedure, since the curvatures of these plots are not known. To minimize this ambiguity, the extrapolation is expediently performed on several $\Delta\epsilon/\epsilon$ values obtained at higher fields by the linear least-squares method. The choice of these $\Delta\epsilon/\epsilon$ values introduces a further uncertainty; thus, only a practical range can be estimated for $(\Delta\epsilon/\epsilon)_s$, as indicated with solid and dashed lines in each plot. The upper limit of $(\Delta\epsilon/\epsilon)_s$ is in the range between 0.362 (five observed $\Delta\epsilon/\epsilon$ points included) and 0.308 (eight points) from the $\Delta\epsilon/\epsilon$ vs. E^{-1} plot, while the lower limit is between 0.266 and 0.235 from the $\Delta\epsilon/\epsilon$ vs. E^{-2} plot. As modus operandi, a simple average of these limits has sometimes been employed for $(\Delta\epsilon/\epsilon)_s$;[18] thus, $(\Delta\epsilon/\epsilon)_s$ = 0.293 at 208 nm for $[Glu(OMe)]_n$ in HFP.

Another procedure for evaluating the $(\Delta\epsilon/\epsilon)_s$ value is the curve-fitting method, by which experimental $\Delta\epsilon/\epsilon$ values plotted against E^2 are fitted to one of theoretical orientation functions, $\Phi(\beta,\gamma)$.[24,27,32] A difficulty involved in this curve fitting is that the weight- or number-average orientation functions must be utilized for a synthetic polymer sample, because it is usually polydisperse regarding the molecular weight of solute.[20,35] In order to calculate such functions for long, rodlike helices, the following parameters must be available:[20,35] the molecular length distribution, the degree of polydispersity in terms of weight-average to number-average molecular lengths, l_w/l_n, the weight-average molecular length, l_w, and the ratio of the weight-average permanent

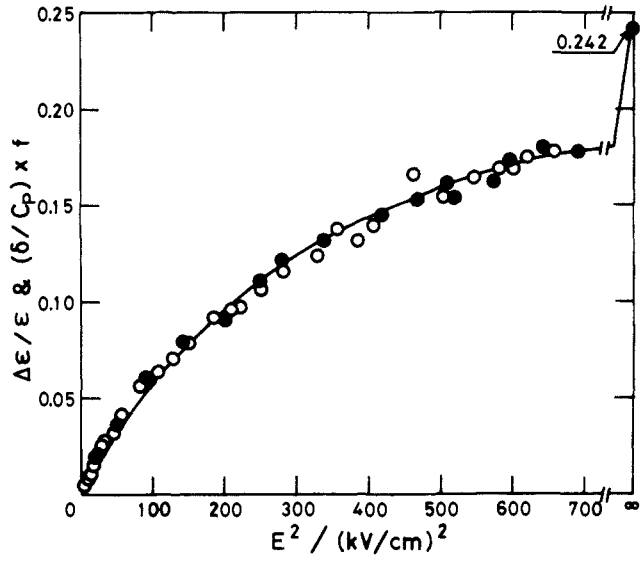

Figure 5. Curve fitting of $\Delta\epsilon/\epsilon$ values at 208 nm to theoretical orientation function: (●) $\Delta\epsilon/\epsilon$ at 208 nm; (○) δ/C_p at 535 nm (deg/M) multiplied by factor $f = 2.442 \times 10^{-5}$; (—) the theoretical curve calculated for the 0.49 mM solution with the parameters[22] l_w = 1190 Å, l_w/l_n = 1.08, $\beta_w^2/2\gamma_w$ = 2.0, and the Lansing–Kraemer distribution function.

manent dipole moment to the weight-average polarizability anisotropy, $\beta_w^2/2\gamma_w$. Fortunately, these quantities have already been evaluated for $[Glu(OMe)]_n$ in HFP in a previous reversing-pulse electric birefringence study.[22] The weight-average orientation functions have also been calculated for the 0.49–7.8 mM $[Glu(OMe)]_n$ solutions.[22] Without going into details, the result will be applied to the present ELD data.

Figure 5 shows the electric field dependence of $\Delta\epsilon/\epsilon$ measured at 208 nm for the 0.50 mM solution (cf. Figure 3b) and the optical phase retardation per residue concentration, δ/C_p, at 535 nm for a 0.49 mM solution (cf. Figure 2 of ref 22). The birefringence values were adjusted by multiplying a constant so that both $\Delta\epsilon/\epsilon$ and δ/C_p nearly coincide with each other over a field strength range 0–26.3 kV/cm. This coincidence indicates that these two types of electrooptical measurements with different instruments were executed properly. These experimental points were fitted to the theoretical orientation function with a $\beta_w^2/2\gamma_w$ of 2 (solid line). The fitting is excellent, particularly over a medium-to-high field strength range. The saturated value at infinitely high field, $(\Delta\epsilon/\epsilon)_s$, was read off to be 0.242 at 208 nm, which is located between two extreme values obtained by the above extrapolation method. The value of 0.242 was adopted in this work; needless to say, it is more reliable than the simple mean of 0.293. It is now possible to evaluate the orientation factor Φ, i.e., the average degree of orientation, for $[Glu(OMe)]_n$ helices at a constant field strength of 17.8 kV/cm: Φ at 17.8 kV/cm = [$(\Delta\epsilon/\epsilon)$ at 17.8 kV/cm]/[$(\Delta\epsilon/\epsilon)$ at saturation] = 0.134/0.242 = 0.554. Remembering that this value, evaluated at 208 nm, is independent of wavelength, we can finally calculate the $(\Delta\epsilon/\epsilon)_s$ values over the entire wavelength region with the aid of eq 3.

The value of 0.242 for $(\Delta\epsilon/\epsilon)_s$ at 208 nm seems to be in good accord with the polarization result of stretched $[Glu(OMe)]_n$ film by Gratzer et al.;[10] their spectra give values of 0.75 for $A_\parallel$ and 0.60 for $A_\perp$ at 208 nm (cf. Figure 3 of ref 10). If eq 1 is assumed to hold for the stretched film (no proof was given in ref 10, however), the $\Delta A/A$ value can be calculated to be 0.231. This value may be approximated to be the saturated value, i.e., $(\Delta A/A)_s$, considering the high molecular weight (8×10^5) and the claimed high orientability of the $[Glu(OMe)]_n$ film. Since the uncertain scattering background and other experimental difficulties are associated with film dichroism,[10] the agreement may be only apparent; nevertheless, it is encouraging and worth mentioning here.

Decomposition of Isotropic Absorption Spectrum and Simulation of Reduced Dichroism Spectrum. Figure 6 shows the saturated

(32) Charney, E.; Yamaoka, K. *Biochemistry* **1982**, *21*, 834–842.
(33) Hogan, M.; Dattagupta, N.; Crothers, D. M. *Proc. Natl. Acad. Sci. U.S.A.* **1978**, *75*, 195–199.
(34) Lee, C.-H.; Charney, E. *J. Mol. Biol.* **1982**, *161*, 289–303.
(35) Yamaoka, K.; Fukudome, K. *Bull. Chem. Soc. Jpn.* **1983**, *56*, 60–65.

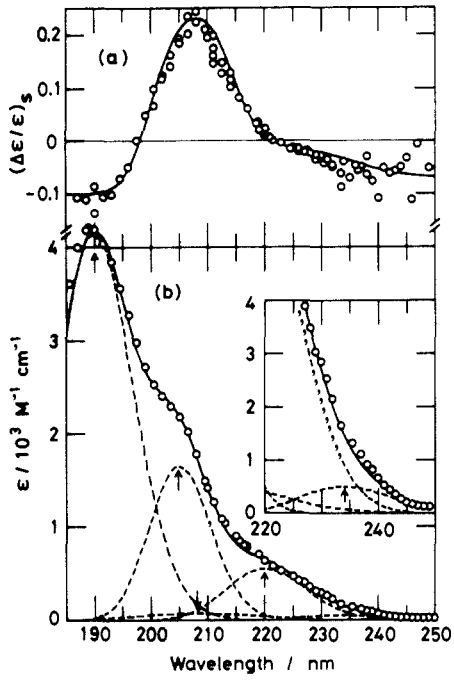

Figure 6. (a) Dependence of saturated reduced dichroism $(\Delta\epsilon/\epsilon)_s$ on wavelength and (b) decomposition of isotropic absorption spectrum into component bands: (○) experimental points. The simulated $(\Delta\epsilon/\epsilon)_s$ spectrum (—) is seen in (a). The decomposed component bands (---) with arrows indicating the peak positions and the resultant isotropic spectrum (—) are seen in (b). The ordinate scale of inset is given by $\epsilon/10^2$.

reduced dichroism and the isotropic absorption spectrum of $[Glu(OMe)]_n$ (circles). It is now possible, for the first time, to quantitatively interpret the absorption spectrum of the peptide chromophore in terms of individual component bands, whose transition moments make some fixed angles with respect to the helix axis. The decomposition of the observed absorption spectrum was carried out, with the assumptions that (1) the ith component band ϵ_i with polarization angle θ_i can be expressed as a Gaussian in terms of wavenumber $\tilde{\nu}$ and (2) the absorption spectrum should be synthesized with the least number of such component bands

$$\epsilon_i(\tilde{\nu}) = \epsilon_{i,max}(\tilde{\nu}) \exp\{-(4 \ln 2)[(\tilde{\nu} - \tilde{\nu}_{i,max})/\delta_i(\tilde{\nu})]^2\} \quad (4)$$

where $\epsilon_{i,max}(\tilde{\nu})$ is the absorption coefficient at $\tilde{\nu}_{i,max}$ and $\delta_i(\tilde{\nu})$ is the half-intensity bandwidth for the ith component band.

The contribution from the side-chain carboxy methyl ester of $[Glu(OMe)]_n$ to the peptide absorption was estimated with *n*-butyric acid methyl ester. This spectrum shows a weak band (ϵ_{max} = 71 M^{-1} cm^{-1} at 204 nm) due to an n–π^* transition, which could be expressed by a Gaussian profile. Similar spectra were obtained for polyacrylic acid at pH 4.13 (ϵ_{max} = 115 at 208–210 nm) and poly(methyl acrylate) in HFP (ϵ_{max} = 124 at 208 nm). The intensity and peak position of the carboxyl or the methyl ester in these polymers are close to those found for *n*-butyric acid ester, which may, therefore, be considered to be the side chain of $[Glu(OMe)]_n$.

The isotropic spectrum of $[Glu(OMe)]_n$ was decomposed into component bands so as to give the least standard deviation (Figure 6b). The peptide band contains at least four components in the 187–250-nm region, exclusive of the side-chain band at 204–210 nm whose contribution is negligibly small. From the longer wavelength side, the first component at 234 nm (band 1) is very weak in intensity and unraveled, for the first time, in this work with some confidence. The locations of the second to fourth components are visually identifiable, as often reported previously.[2,10,16,36] The fifth band may exist near 180 nm,[36] as already suggested in a vacuum CD study,[37] but the $\Delta\epsilon/\epsilon$ behavior in

Table I. Optical Parameters Characteristic of Component Bands Involved in the 187–250-nm Absorption Spectrum of $[Glu(OMe)]_n$

band i	$\lambda_{i,max}$/nm	$\epsilon_{i,max}/M^{-1}$ cm^{-1}	δ_i/cm^{-1}	$\lvert\theta\rvert_i$/deg	f_i[a]
1	234.0	50	3400	55.60 (56.20)[b]	0.00078
2	220.0	540	3400	54.73 (54.80)	0.00844
3	204.9	1650	3000	50.60 (49.00)	0.0228
4	190.0	4150	4270	56.10 (56.80)	0.0815
CO_2Me[c]	208.0[d]	69	6000	58.0[e] (58.0)[e]	0.00190

[a] The oscillator strength defined as $f = 4.319 \times 10^{-9} \int_0^\infty \epsilon(\tilde{\nu})\, d\tilde{\nu}$. [b] In this column, the angles in parentheses were calculated with the highest possible extrapolation value of 0.362 for $(\Delta\epsilon/\epsilon)_s$. [c] The absorption spectrum of *n*-butyric acid methyl ester in HFP fitted by a Gaussian profile. [d] The position may be shifted between 204 and 208 nm, but such a shift does not affect the resultant absorption spectrum, if ϵ_{max} remains to be ca. 70. [e] This angle may be varied from 54.7 to 90°, but 58° gives a good fit.

Figures 2 and 6 allows no clear-cut conclusion at present. An extension of the ELD work to the shorter wavelength region is needed. The parameters characteristic of each component band are given in Table I. It is interesting to note that the values of oscillator strength are 0.0815 for the 190-nm band and 0.0228 for the 205-nm band, the ratio being 3.6. Mandel and Holzwarth found the ratio of dipole strengths to be 4.94.[16] With many adjustable parameters, the decomposition in Figure 6b may not be claimed to be unique. Yet, these parameters are reliable, because both ϵ_i and λ_i values (i = 1–4) must be used without any tolerance to reproduce the wavelength dependence of $(\Delta\epsilon/\epsilon)_s$ successfully (see below). The peak positions are surprisingly in good agreement with the CD result of $[Glu(OMe)]_n$ in HFP.[30] The isotropic absorption spectrum (solid line) was stimulated from the component bands (broken lines). The general trend was not affected by a weak side-chain (CO_2Me) band, though this was included at 208 nm. The simulated spectrum agrees quite well with the one experimentally obtained in the absence of applied electric field (circles).

The wavelength dependence of $(\Delta\epsilon/\epsilon)_s$, i.e., the $(\Delta\epsilon/\epsilon)_s$ spectrum, is now simulated by substituting in eq 3 and 4 the parameters for the peptide and side-chain bands given in Table I. The angle θ_i is chosen on a trial-and-error basis, but the freedom of choice is quite limited because of the predetermined parameters for the component bands. The result is shown in Figure 6a, where the agreement between the simulated (solid line) and experimental (circles) $(\Delta\epsilon/\epsilon)_s$ spectra is excellent over the entire wavelength region. The most probable angles are given in Table I. It should be emphasized that these angles are unexpectedly different from the theoretically predicted values (see later discussion).[6,7] The maximum value of 0.242 for $(\Delta\epsilon/\epsilon)_s$ at 208 nm is a sandwich effect by three overlapping components (bands 2–4). It has already been reported that poly(γ-benzyl L-glutamate) shows ELD signals for which the side-chain benzyl group is responsible.[12] In the case of $[Glu(OMe)]_n$, the addition of the carboxy methyl ester band with an angle (θ_{CO_2Me}) larger than 54.7° improves slightly the wavelength dependence of $\Delta\epsilon/\epsilon$ between 208 and 220 nm in Figure 6a.

In order to see how angles θ_i alter with the value of $(\Delta\epsilon/\epsilon)_s$, the highest value of 0.362, obtained from the $\Delta\epsilon/\epsilon$ vs. E^{-1} plot (cf. Figure 4), was assigned for $(\Delta\epsilon/\epsilon)_s$, and the $(\Delta\epsilon/\epsilon)_s$ spectrum was simulated. The best estimated angles were also given in Table I. Although an extremely high value of $(\Delta\epsilon/\epsilon)_s$ was used, these angles remained nearly the same as those evaluated with the $(\Delta\epsilon/\epsilon)_s$ of 0.242. Hence, the conclusion on polarization angles is unaffected.

Polarization Directions of Peptide Bands. According to Moffitt's prediction,[6,7] the peptide chromophores in an infinitely long helix should give rise to only two allowed absorption bands for the 190-nm π–π^* transition, the parallel (∥) and perpendiular (⊥) components. In previous experiments,[8-11,16,31,36] the 190- and 205-nm component bands have been assigned to be ⊥ and ∥

(36) Quadrifoglio, F.; Urry, D. W. *J. Am. Chem. Soc.* **1968**, *90*, 2755–2760.

(37) Johnson, W. C., Jr.; Tinoco, I., Jr. *J. Am. Chem. Soc.* **1972**, *94*, 4389–4390.

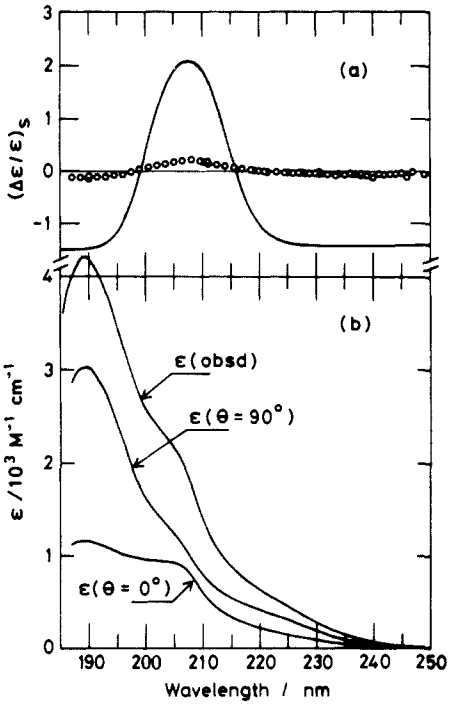

Figure 7. (a) Simulation of saturated reduced dichroism $(\Delta\epsilon/\epsilon)_s$ based on Moffitt's prediction and (b) decomposition of isotropic absorption spectrum ϵ(obsd) into the parallel, $\epsilon(\theta = 0°)$, and perpendicular, $\epsilon(\theta = 90°)$, component bands with non-Gaussian band profiles: (a) simulated (—) and observed (○); (b) bands 1, 2, and 4 taken as perpendicular ($\theta = 90°$) and band 3 as parallel ($\theta = 0°$). In (a) and (b), the contribution from the side chain of $[Glu(OMe)]_n$ was ignored.

polarized relative to the helix axis. If this assignment is correct, the angles should be 90° for θ_4 (the 190-nm band) and 0° for θ_3 (the 205-nm band). With these angles being substituted in eq 3, together with ϵ_i (i = 1–4) and an angle of 90° tentatively abopted for bands 1 and 2, $(\Delta\epsilon/\epsilon)_s$ values were calculated between 185 and 250 nm. The result is shown in Figure 7a with solid line; clearly, the calculated wavelength dependence differs from the observed one (circles) far beyond experimental errors. On the pretext of the least number for component bands with Gaussian band profile, the angles θ_i (i = 3,4) can be neither 90° nor 0° relative to the axis of orientation, that is, the helix axis. Hence, our ELD results, analyzed under the above conditions, do not support Moffitt's concept of band splitting.

An alternative test of the validity of Moffitt's band split is based on the relaxation of the constraint of Guassian band shape for the ∥ and ⊥ components. The isotropic absorption spectrum should then be decomposed into the ∥ ($\theta_3 = 0°$) and ⊥ (θ_2 and $\theta_4 = 90°$) components, wavelength by wavelength, with the aid of eq 3 in such a way that the simulated reduced dichroism coincides with the experimental $(\Delta\epsilon/\epsilon)_s$ values in the 187–250-nm region. The result is shown in Figure 7b. Both the decomposed ∥- and ⊥-component bands now overlap strongly with each other over the entire wavelength region. The band shapes are considerably broad and ill-defined; for example, the molar absorption coefficient of the ⊥ band is about 1.4 times larger than that of the ∥ band even at the 205-nm peak. At the observed 190-nm peak, the ⊥ band is not pure either, strongly overlapping with the ∥ band. The band shapes for these ∥ and ⊥ components are unrealistic, having extraordinarily wide half-intensity bandwidths. In order to interpret the 187–250-nm peptide band in terms of the split ∥ and ⊥ components, a non-Gaussian band profile had to be assumed, but the result proved to be an overlap of, rather than a split into, two bands, each appearing to be a composite of several subbands. Hence, the present ELD experimental result contradicts Moffitt's prediction.

$(\Delta\epsilon/\epsilon)_s$ Spectra and Polymer Conformations. The helical conformation of $[Glu(OMe)]_n$ in HFP and other helix-forming solvents undoubtedly belongs to the α-helix group[16,24,25,30,36–39] in which both α- and ω-helices are well-defined.[40,41] It has been pointed out that the $[Glu(OMe)]_n$ helix in solution is *soft*[16] or susceptible to an external electric field.[24] It was recently shown that this helix undergoes an electric field induced helix-to-helix transition in the course of field orientation.[22,23] The new helix was stable, once formed, returning to the original helix on removal of the field; the transition was completely reversible. The transition was concluded to be the conformational change from α- to ω-helices.[22] The helical array of peptide groups around the helical axis differs only slightly between α- and ω-helices.[41] Thus, the peptide chromophore understandably gives rise to the field-on and field-off absorption spectra, which are close to each other, as indicated in the inset of Figure 2 (bottom). It is safe to conclude that the $(\Delta\epsilon/\epsilon)_s$ spectrum in Figure 6 is a representative one for the α-helix group.

An additional fact to be emphasized here is that $(NaGlu)_n$[17] and poly(L-ornithine perchlorate)[42] in the random-coiled conformation give rise to the $(\Delta\epsilon/\epsilon)_s$ spectra quite similar to those of $(Glu)_n$[17] and $[Glu(OMe)]_n$ in the helical conformation. It should also be pointed out that the $(\Delta\epsilon/\epsilon)_s$ spectrum of triple-helix collagen molecules gives rise to the same features as observed for $(Glu)_n$ and $[Glu(OMe)]_n$.[18]

Peptide Bands Inferred from Reduced Dichroism. The weak, longest wavelength band near 234 nm (band 1, $\epsilon_1 \approx 50$) is probably due to an n–π* transition under consideration of the intensity. Among others, Parrish and Blout noted that a weak negative CD band at 238 nm of unknown origin may be present in the *random-coiled* $(NaGlu)_n$ at a pH of 7.[30] Indeed, a large number of reports show or describe this CD band, which has so far been observed only in random-coiled polypeptides. The CD band is, however, not confined to $(Glu)_n$[43,44,46,47,50] and its derivatives[30,43,46,47,50] but also appears in poly(L-lysine)[45–47,51] and the homologues containing amino side chains[51] and in copolymers.[48,49] The fact that poly(L-lysine) shows such a weak CD band decisively rules out the possibility that it is due to the side-chain carboxyl group. Hence, the 234-nm band in Figure 6 should be attributed to an optical transition from one of the electrons on the peptide oxygen atom.[52] The reason that this weak negative CD band has not been observed in the CD spectrum of helical polypeptides may be explained as being due to an overlap by the strongly negative 222-nm CD band. Here, the advantage of ELD measurements over isotropic CD spectra is evident.

The second, weak component (band 2) with an ϵ_{max} of 540 at 220 nm corresponds to the strong negative CD band, which has been assigned to *the n–π* transition*.[2] This is probably correct, though the absorption intensity is higher than ordinary n–π* transitions.[53] Since the angle θ_2 is ±54.73°, the transition moment direction is not perfectly perpendicular or normal to the helix axis of $[Glu(OMe)]_n$, if the peptide planes (the carbonyl groups) lie nearly parallel to the helix axis.[41] The peptide planes can be expressed with the tilt and twist angles relative to the helix axis,

(38) Ishimuro, Y.; Yamaguchi, S.; Hamada, F.; Nakajima, A. *Biopolymers* **1981**, *20*, 2499–2508.
(39) Cassim, J. Y.; Yang, J. T. *Biopolymers* **1970**, *9*, 1475–1502.
(40) Bamford, C. H.; Elliott, A.; Hanby, W. E. *Synthetic Polypeptides*; Academic: New York, 1956.
(41) Dickerson, R. E.; Geis, I. *The Structure and Action of Proteins*; Harper & Row: New York, 1969; Chapter 2, pp 24–33.
(42) Yamaoka, K.; et al., manuscript in preparation. The ELD result of poly(L-ornithine perchlorate) at pH 6.0 is similar to that of random-coiled $(NaGlu)_n$ at pH 6.9.[17]
(43) Adler, A. J.; Hoving, R.; Potter, J.; Wells, M.; Fasman, G. D. *J. Am. Chem. Soc.* **1968**, *90*, 4736–4738.
(44) Tiffany, M. L.; Krimm, S. *Biopolymers* **1969**, *8*, 347–359.
(45) Greenfield, N.; Fasman, G. D. *Biochemistry* **1969**, *8*, 4108–4116.
(46) Tiffany, M. L.; Krimm, S. *Biopolymers* **1972**, *11*, 2309–2316.
(47) Tiffany, M. L.; Krimm, S. *Biopolymers* **1973**, *12*, 575–587.
(48) Rippon, W. B.; Chen, H. H.; Walton, A. G. *J. Mol. Biol.* **1973**, *75*, 369–375.
(49) Rippon, W. B.; Hiltner, W. A. *Macromolecules* **1973**, *6*, 282–285.
(50) Rinaudo, M.; Domard, A. *J. Am. Chem. Soc.* **1976**, *98*, 6360–6364.
(51) Tseng, Y.-W.; Yang, J. T. *Biopolymers* **1977**, *16*, 921–935.
(52) Caldwell, D. J.; Eyring, H. *Annu. Rev. Phys. Chem.* **1964**, *15*, 281–310.
(53) Barnes, D. G.; Rhodes, W. *J. Chem. Phys.* **1968**, *48*, 817–824.

if these angles are available, as in the case of the DNA double helix. Then, the angles θ_i found in this work can be related to the *rotational* angles of the transition moments around an axis perpendicular to the peptide plane.[54] We will correlate the angles θ_i with various helical conformations in future work.

Concluding Remarks. By the reversing-pulse electric birefringence method, the rotational relaxation time $\langle\tau\rangle_{EB}$, of the present $[Glu(OMe)]_n$ sample was evaluated from field-off decay curves in HFP under the same experimental conditions.[22] The axial translation per residue of the $[Glu(OMe)]_n$ helix backbone was then found to be 1.56 Å with the Broersma equation for the rodlike molecule.[22] On this basis, it was concluded that the tertiary winding of the helical chain was probably insignificant and that the conformation was α-helical. Hence, the observed polarization angles of peptide chromophores cannot be attributed to the overall molecular flexibility. The analysis of the $(\Delta\epsilon/\epsilon)$ spectrum of $[Glu(OMe)]_n$ clearly shows that the 190- and 205-nm bands are not polarized either perpendicular or parallel to the helix axis, as originally predicted by a simple exciton theory.[6,7] Furthermore, the intensity ratio of these two bands is about 3.3 (cf. Table I of the present work) or 4.9 (Table I of ref 16) in terms of the dipole strength, a marked contrast with theoretically calculated values of 1.66-1.38, as noted by Mandel and Holzwarth.[16] We ask what then are the alternative assignments of those component bands. The absorption spectra of small amide compounds are quite complex, and the number of transitions is still uncertain. Although the amide band at 180-210 nm has been assigned to a single π-π^* transition, this view is by no means unanimous, as reviewed by Woody.[2] For instance, it has amply been demonstrated that an intermediate band is present for substituted amides between the strong 190-nm and weak 220-nm bands in the gas phase.[53,55-57] If such a band is also identified in the condensed phase, then the splitting of the peptide band in the helical conformation should be reappraised. Thus, before we reach any final conclusion on the peptide band splitting, the present line of ELD studies must be extended to other helical polypeptides on one hand, and film dichroism studies must also be carried out for oligomeric peptides and small amides on the other.

Registry No. Poly(γ-methyl L-glutamate) (homopolymer), 25086-16-2; poly(γ-methyl L-glutamate) (SRU), 25036-43-5.

(54) Matsuoka, Y.; Nordén, B. *Biopolymers* **1982**, *21*, 2433-2452.

(55) Basch, H.; Robin, M. B.; Kuebler, N. A. *J. Chem. Phys.* **1967**, *47*, 1201-1210.

(56) Basch, H.; Robin, M. B.; Kuebler, N. A. *J. Chem. Phys.* **1968**, *49*, 5007-5018.

(57) Kaya, K.; Nagakura, S. *J. Mol. Spectrosc.* **1972**, *44*, 279-285.

Biosynthesis of the Kinamycin Antibiotics by *Streptomyces murayamaensis*. Determination of the Origin of Carbon, Hydrogen, and Oxygen Atoms by ^{13}C NMR Spectroscopy†

Yukiharu Sato‡ and Steven J. Gould*[1]

Contribution from the Department of Chemistry, Oregon State University, Corvallis, Oregon 97331. *Received December 9, 1985*

Abstract: Feeding of $[1,2\text{-}^{13}C_2]$acetate to cultures of *Streptomyces murayamaensis* gave kinamycin C and kinamycin D, each showing intact incorporation of acetate at carbons 1/2, 3/4, 10/5, 6/7, 8/9, 6'/1', 2'/CH_3, and 4'/5' and at the esters, as well as simple enrichment in C-3', as shown by ^{13}C NMR analysis. The orientation of each acetate in kinamycin D was revealed by incorporation of $[1\text{-}^{13}C,2,2,2\text{-}^{2}H_3]$acetate. ^{13}C NMR analysis indicated enrichment at carbons 1, 3, 6, 8, 10, 2', 4', and 6' and the ester carbonyls; isotope-shifted resonances were also observed for carbons 6, 10, and 2' and the ester carbonyls, indicating retention of deuterium at the adjacent positions from the original acetate. Thus, the biosynthetic origin of all the carbons of kinamycin, except the cyano moiety, was revealed. When $[1\text{-}^{13}C,1,1\text{-}^{18}O_2]$acetate was fed, isotope-shifted peaks were observed for carbons 1, 8, and 4' and the ester carbonyls of kinamycin C and of kinamycin D, indicating retention of ^{18}O at these positions, and when kinamycin D was produced in the presence of $^{18}O_2$, isotope-shifted peaks were observed for carbons 4, 1', and 2'. These results are consistent with the kinamycin skeleton being derived from acetate via 1,3,8-trihydroxynaphthalene—subsequently oxidized either to 2-hydroxyjuglone or to juglone—and 4-amino-2-hydroxytoluic acid. The D ring is most reasonably generated by oxidation of tetracyclic intermediate **18b** to hydroquinone **19b** and then to epoxide **20b**, followed by rearrangement to epoxyquinol **21**, reduction, and epoxide opening with trans attack by water.

The kinamycins [A-D (**1-4**, respectively)] are a group of antibiotics produced by *Streptomyces murayamaensis* sp. nov. Hata and Ohtani that were isolated and characterized by Omura et al.[2,3] The structures were determined in part by chemical and spectroscopic means.[4] The complete structure of kinamycin C (**3**) was obtained from an X-ray crystallographic study,[5] and its relationship to the others was subsequently confirmed.[6] Thus, these metabolites contain highly novel features: a benzo[*b*]tetrahydrocarbazole skeleton and an *N*-cyano moiety. We recently published the complete assignments of the ^{13}C and ^{1}H NMR spectra of kinamycin D (**4**).[7]

The kinamycins are strongly active against Gram-positive bacteria, but less so against Gram-negative organisms.[3] The antimicrobial activity increases inversely with the number of acetates present. Periodate degradation of the D ring of the

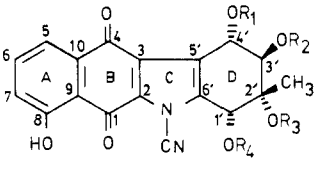

	R_1	R_2	R_3	R_4
1	H	Ac	Ac	Ac
2	H	H	Ac	H
3	Ac	Ac	H	Ac
4	H	Ac	H	Ac

† Dedicated to Professor George H. Büchi on the occasion of his 65th birthday.

‡ On leave from Tamagawa University, 6-1-1 Tamagawa Gakuen, Machida-shi, Tokyo 194, Japan.

0002-7863/86/1508-4625$01.50/0